Int. J. Electrochem. Sci., 11 **(2016)** 5380 – 5394, doi: 10.20964/2016.07.39

International Journal of
ELECTROCHEMICAL
SCIENCE
www.electrochemsci.org

One-step Electrochemical Synthesis of Polyaniline/Metallic Oxide Nanoparticle (γ-Fe_2O_3) Thin Film

Cleiser Thiago Pereira da Silva[1], *Vicente Lira Kupfer*[1], *Genilson Reinaldo da Silva*[1], *Murilo Pereira Moisés*[1,2], *Magno Aparecido Gonçalves Trindade*[3], *Nelson Luis de Campos Domingues*[3], *Andrelson Wellington Rinaldi*[1*]

[1] Materials Chemistry and Sensors Laboratory – LMSen, State University of Maringa – UEM. Chemistry of Department, Av. Colombo 5790, CEP: 87.020-900, Maringá-PR, Brazil.
[2] Federal Technological University of Paraná – UTFPR, CEP 86812-460, Apucarana-PR, Brazil.
[3] Federal University of Grande Dourados - UFGD, CEP: 79.804-970, Dourados-MS, Brazil.
[*]E-mail: andrelson.rinaldi@gmail.com; awrinaldi@uem.br

Received: 15 February 2016 / *Accepted:* 4 May 2016 / *Published:* 4 June 2016

Polyaniline and metallic oxide (γ-Fe_2O_3) composite thin film was simultaneously synthesized using an electrochemical technique in a solution containing aniline, oxalic acid, and iron(III) sulfate in an alkaline medium. The results of the reaction process, which was monitored using infrared spectra at a specific wavelength of 638 cm^{-1} along with an X-ray diffractogram of the respective angles 30.6^o, 35.4^o, and 60.7^o 2 θ degree, indicated the presence of (γ-Fe_2O_3) and polyaniline in a single step. UV-Vis spectra suggested that the metal oxide interacted synergistically with the quinoid and benzoid groups, with absorption of approximately 560 nm and 280 nm present in the polymeric matrix. Thermogravimetric analysis (TGA) of the composite lost 10% of the weight at approximately 188^{o}C. Together with TEM images, the results showed that iron oxide particles are nanometer-sized (126 ± 30 nm). Furthermore, SEM images show that multiple cycles of synthesis modify the mechanical properties of films prepared simultaneously with (γ-Fe_2O_3). The voltammetric behavior of the composite showed a reversible process. Furthermore, a preliminary test showed that our material has the potential to be applied in gas sensors.

Keywords: Composites; Nanostructures; Structural materials; Electrochemical properties; Electrochemical measurements.

1. INTRODUCTION

There are many extant studies about the synthesis of composites that contain conducting polymers (polythiophene, polypyrrole, *o*-anisidine, and polyaniline), but polyaniline (PANI) is the polymer that has been investigated the most in the literature [1-5]. Facility doping, low cost of raw materials, processability, and environmental stability are the characteristics that make PANI the most attractive conducting polymer [2,6]. Studies of the composites that comprise PANI and metal oxides, such as WO_3 [7], Fe_2O_3 [8], ferrites [9], and titanium oxide [10] are very well documented. These materials can be used in devices such as photovoltaic cells [11], catalysts [12], and sensors for electroanalysis [13,14], etc. Synthesis routes have also been reported, such as traditional *in situ* polymerization [15], microwave-assisted polymerization [16], polymerization assisted by UV light [17] and electrochemical polymerization [18]. However, in all these studies, the synthesis methods are conducted in acid media, and the metal oxide must be previously prepared using the *Pechini* [19], sol gel [20], and/or *inter alia* techniques.

The simultaneous synthesis of materials has been explored by various researchers. Zhu *et al.* [21] prepared PANI-intercalated layered vanadium oxide nanocomposites, with a thickness of between 10 – 20 nm and a typical lateral dimension in the range of hundreds of nanometers to several micrometers. Mumtaz *et al.* [22] synthesized material hybrid PEDOT–metal latexes.

The literature presents little discussion about electronic conducting polymers synthesized in an alkaline solution. Zhou *et al.* [23] chemically synthesized PANI via chemical methods in strong alkaline aqueous solutions at different temperatures. The authors found that the PANI synthesis and morphology were significantly influenced by NaOH concentration and temperature. However, the authors did not achieve an identification of the electrogenerated products. Peng *et al.* [24] synthesized PANI by electrochemical means across a broad pH range, showing that it is possible to synthesize polyaniline in alkaline media. The electrochemical synthesis of poly-*o*-anisidine and metallic oxide (Fe_2O_3), in a nanometric size, was studied by Fonseca *et al.* [3] using electropolymerization at the Pt electrode surface in alkaline media and using an amperometry technique. Previous studies [25] from our group reported the synthesis of PANI doped with citric acid (Fe_2O_3) in an alkaline medium in which it was possible to obtain the composite thin film synthesis in on step. The properties of the material obtained were excellent compared to the precursors; furthermore, the process of electrochemical synthesis without the presence of polymeric beads, colloids, and/or emulsions remains under-explored in the literature, though it has the potential for a very broad application.

The composite thin film, PANI, doped with Fe_2O_3 is well known. However, the simultaneous synthesis of composite thin film in alkaline media opens the doors to obtaining known composites with improved properties. Therefore, the aim of this work was to report the simultaneous synthesis of PANI and metallic oxide (γ-Fe_2O_3) thin film in alkaline media. The electrochemical technique was used to electropolymerized this thin film onto the platinum electrode from mixed solutions containing aniline, oxalic acid (OA), and $Fe_2(SO_4)_37H_2O$. It is noteworthy that the material exhibited a response to the percentage of ethanol/water; this behavior indicates that hybrid material has the potential to be used as a sensor in the ethanol/water mixture.

2. EXPERIMENTAL

2.1 Chemical and Material

Aniline monomer (JTBaker) was previously distilled in a nitrogen atmosphere, with metallic zinc, before use. Ferric sulfate and OA, sodium hydroxide, and hydrochloric acid (Sigma Aldrich) were used as received. Ultra-pure Milli-Q water was used for the preparation of all the solutions, and other reagents had a purity of type P.A.

2.2 Synthesis of composite thin films

The synthesis of the materials was prepared according to Silva *et al*. [25]. Briefly, two solutions, with the pH adjusted to 9.0, were prepared for the synthesis of the respective composites. First, a solution containing 0.1 mol/L OA and aniline monomer was electropolymerized and the composite thin film prepared from this solution was called PANI/OA. Another solution with 0.1 mol/L OA, aniline monomer, and iron(III) sulfate was also electropolymerized and the resulting composite thin film was called PANI/OA/γ-Fe_2O_3. The synthesis was carried out at room temperature. A potentiostat/galvanostat PGSTAT-302 N (Autolab, Eco Chemie). A three-electrode setup was used, as well as an electrochemical cell system, to synthesize the materials.

A platinum plate or PET/ITO substrate was used as the work electrode, a large area platinum plate was used as the counter electrode, and a saturated calomel electrode (SCE) was used as the reference electrode. The platinum plates were cleaned in Piranha solution (sulfuric acid/hydrogen peroxide 3:1) for 30 min, and then rinsed with ethanol and water in abundance before electropolymerization of the material onto the electrode surface was performed and electrochemical measurements were taken.

The synthesis of the composite thin films PANI/OA and PANI/OA/γ-Fe_2O_3 was carried out using the chronoamperometry technique, in which alternating cycles are applied, and the potential range was between -1.2 V and 1.2 V *vs*. SCE for 4 seconds. These thin film composites were prepared with 5, 10, and 15 cycles. After preparation, the thin films were rinsed with ethanol and water and were characterized.

2.3 Characterizations

Infrared measurements were performed on KBr pellets using JASCO equipment in the region of 400 cm^{-1} to 2000 cm^{-1} with a resolution of 4 cm^{-1} and 256 accumulated spectra. The molecular absorbance spectra were performed with a Varian Cary 50 UV-Vis spectrophotometer in the region of between 230 nm and 800 nm. The polymer solutions were prepared in N-methylpyrrolidone (NMP) at concentrations of 0.1 g/L. The spectra X-ray (XRD) analysis of the films deposited on the PET substrate/ITO were carried out in a Shimadzu model XRD 7000, with a source emission cathode copper current of 30 mA and 40 kV power, a scan range of 10^o to 80°, and a spacing of 2° per min. Thermogravimetric analyses of materials was made through a Shimadzu, model TA50, under N_2, with a flow of 20.0 mL/min and a heating rate of around 10°C/min.

The morphological analysis of the surface characterization was performed using scanning electron microscopy (SEM) with a Shimadzu SSX-550 Superscan Microscope. The transmission electron microscopy (TEM) was performed to determine nanoparticles inside the composites using a Shimadzu JEOL – JEM 1400 Microscope.

The electrochemical characterizations and electrochemical impedance spectroscopy were performed with in an Autolab PGSTAT-302N/FRA using the cyclic voltammetry technique. The electrochemical behavior was made to fall within the potential range of between (-1.0 V and 0.75 V) in solutions of NaOH 1.0 mol/L, at a scan rate of 10, 25, 50, 75, 100, 150, 175, 200, 250, 300, 350, and 400 mV/s.

The electrochemical impedance spectroscopic characterization of the composite was performed at a bias potential of 100 mV, and the studied frequency ranged from 0.1 Hz to 1 MHz. The composite was synthesized in the interdigitated electrodes gold with specifications described elsewhere [26] in the presence of media containing mixed vapors of water and ethanol.

3. RESULTS AND DISCUSSION

3.1 Electropolymerization composite thin films PANI/OA/γ-Fe_2O_3

The synthesis of the PANI composite and iron oxide (γ-Fe_2O_3) was performed by dissolving aniline, $Fe_2(SO_4)_3$, and oxalic acid in aqueous media. Oxalic acid was used to form a complex with Fe(III) ions in an alkaline medium. Moreover, part of the oxalic acid was also used to dope the PANI when electropolymerized. At pH 9.0, the solution presented a reddish coloration. During the electrochemical synthesis, the growth of a thin film of dark coloration on the working electrode was observed. The current (i) *vs* time (s) of chronoamperometry decreased along the deposition time (data not shown). The decrease in the current indicates that the polymeric film increased the number of cycles. The synthesized composite was rinsed with ethanol and water to remove any oligomer.

Figure 1 shows the experimental scheme for the synthesis of the composites.

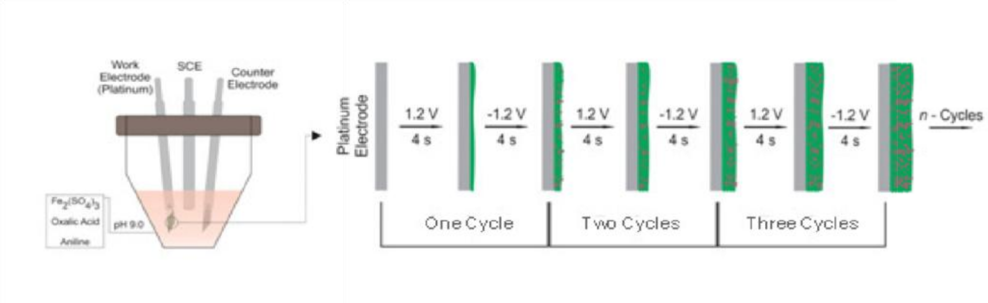

Figure 1. Schema experimental of synthesis simultaneously of composites thin films.

3.2 FT-IR, X-Ray diffraction (XRD), and UV-Vis spectra

The infrared spectra of the composites PANI/HCl, PANI/OA, and PANI/OA/γ-Fe_2O_3 are shown in Figure 2 (a, b). Figure 2 (a) shows that the composite PANI/OA/γ-Fe_2O_3 presented the vibrational stretching modes of aromatic quinoid groups (N=Q=N) 1594 cm^{-1} and benzoid (N=B=N) 1496 cm^{-1}, with a stretching (Q=N=B) in *ca.* 1316 cm^{-1} and aromatic secondary amines (C-N) 1232 cm^{-1}. The signal at 1168 cm^{-1} was assigned to the protonated PANI (N-H). The characteristic peak of protonated PANI shifted to regions of higher wavenumbers, which can be attributed to the interactions between PANI and metal oxide. The low intensity of the signal centered at *ca.* 1168 cm^{-1}, 1232 cm^{-1}, and 1316 cm^{-1} is another relevant factor that also attributed to the interactions between metal oxide and the polymer matrix. Moreover, signals in 1106 cm^{-1} and 1073 cm^{-1} (dashed lines) were attributed to vibrations (S=O). The groups derived from the metal salt in this case, the iron(III) [27] indicate that part of the sulfate solution was incorporated into the composite. The graphic expansion shows details of the signal characteristics of each composite between 800 and 400 cm^{-1} (Figure 2 b).

Moreover, the typical maghemite (γ-Fe_2O_3) signals were observed for wavenumber 776 cm^{-1}, 638 cm^{-1}, 544 cm^{-1}, and 441 cm^{-1} (dashed lines), which is in agreement with the literature [28], although this is mainly true for the signal in 638 cm^{-1}.

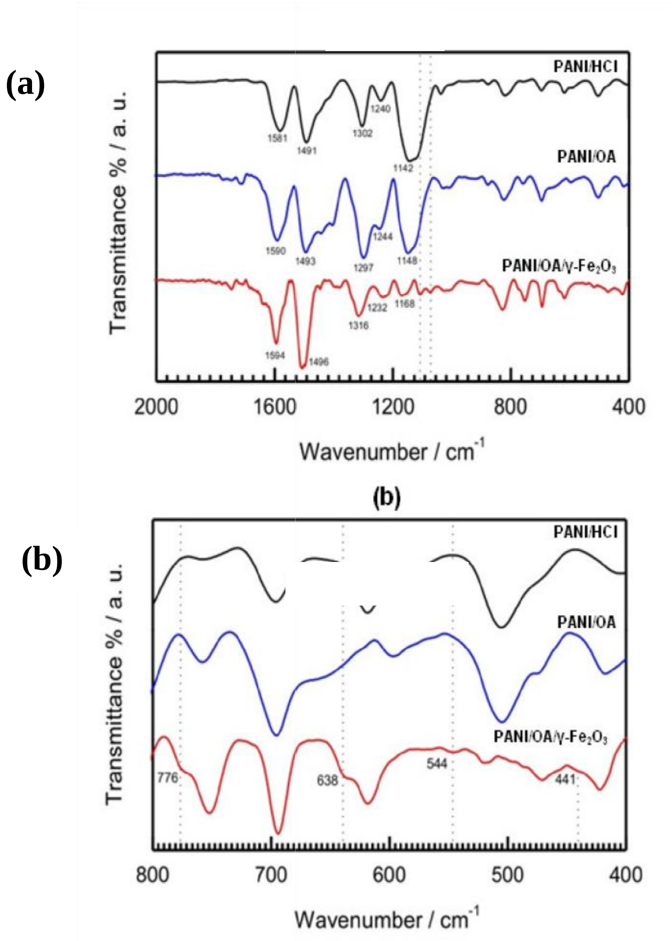

Figure 2. (**a**) FTIR spectra in KBr monitored in the region between 2000 and 400 cm^{-1}. (**b**) FTIR spectra in KBr monitored in the region of 800 to 400 cm^{-1}.

The main signals 30.60^{o}, 35.4^{o}, and 60.7^{o} 2 θ degree, for the (γ-Fe_2O_3) have been observed in the spectra of X-Ray diffraction of the composite (XRD) (**Supplementary Data Figure 1**). Despite the low intensity, these values are in accordance with JCPDS patterns of the main diffraction peaks for maghemite (γ-Fe_2O_3) (JCPDS file, No. 39-1346). Figure 3 (a) shows the UV-vis spectra-monitored in the region of 230 nm to 800 nm for the composite PANI/OA and PANI/OA/ γ-Fe_2O_3. The spectra of PANI/OA had an electronic transition of type (n-π*) in *ca.* 560 nm, and electronic transitions (π-π*) in *ca.* 280 nm. It should also be noted that the composite containing Fe_2O_3 had a low intensity band in

560 nm, while a shift of the band from 280 nm to 302 nm was seen in PANI/AO/γ-Fe_2O_3 compared to the signal presented by PANI/OA.

In accordance with the literature [29], the absorption in the region of *ca.* 630 nm is related to transitions in the polarons quinoid rings, while the absorption in the region of *ca.* 300 nm are related to the benzoid rings. Thus, we suggest that the nanoparticles γ-Fe_2O_3 quinoid interact with the rings decreasing the absorption of light by quinoid rings.

3.3 Thermogravimetric analysis (TGA)

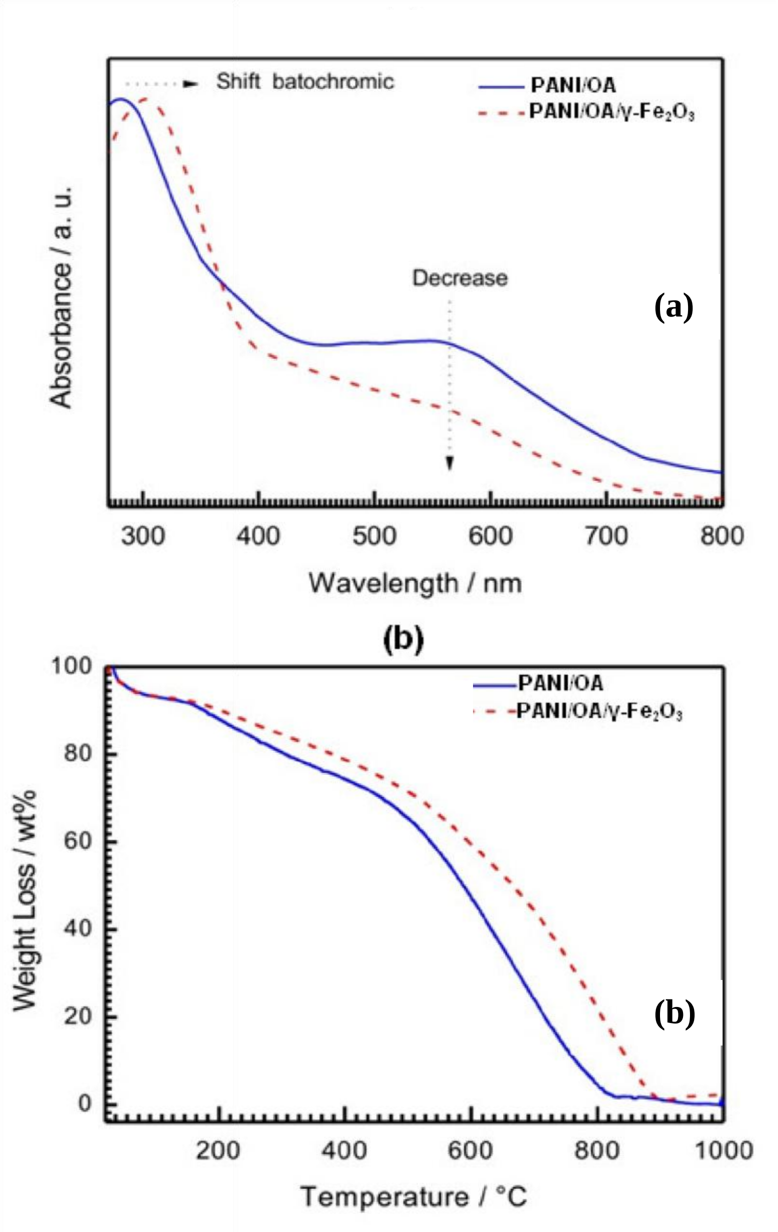

Figure 3. (**a**) UV-Vis spectra of PANI/OA and PANI/OA/γ-Fe_2O_3 in NMP. (**b**) Termogravimetric analysis of PANI/OA and PANI/OA/γ-Fe_2O_3.

The thermogravimetric analysis of the PANI/HCl, PANI/OA, and the composite PANI/OA/γ-Fe_2O_3 are shown in Figure 3 (b). In agreement with the literature [30], it was observed that the pure materials PANI/HCl present weight loss in trees. The PANI lost 10% of its weight at *ca.* 86°C while the materials PANI/OA and PANI/OA/γ-Fe_2O_3 lost the same weight at *ca.* 167°C and 188°C, respectively.

The thermal stability of the polymer increased when the conducting polymer was simultaneously synthesized with γ-Fe_2O_3. The results of the thermogravimetric analysis of the PANI/OA and PANI/OA/γ-Fe_2O_3 suggest that the weight loss of the composite occurs over three different events. The first event indicates that the polymers lose weight at a temperature around 110°C, and this process can be related to the evaporation of the remaining water, which corresponds to *ca.* 5% of the total weight of the composite. The second event is observed between 120 and 450ºC for the PANI/OA, and between 120 and 510ºC for PANI/OA/γ-Fe_2O_3. This event is attributed the component oxalic acid. The third and major event, from 450 to 830°C for PANI/OA and from 510 to 920°C for PANI/OA/γ-Fe_2O_3 was attributed to the destruction of the polymeric backbone. This shows that in the situ polymerization of aniline, the formation of γ-$Fe_2O_{3,}$ particles leads to a better and more thermally stable conducting polymer. It is believed that the increase in thermal properties of the composite thin film can be attributed to the insertion of γ-Fe_2O_3 nanoparticles into the matrix, which provides, besides the polymer-polymer interaction, polymer-NPs.

3.4 Scanning Electron Microscopy (SEM) and Transmission Electron Microscopy (TEM)

The scanning electron micrographs (Figures. 4 a, b, c) of the synthesized PANI/OA polymer films at different synthesis cycles (5, 10, and 15) show that the morphology of the films are homogenous, compact, and have defects in terms of crater shapes. The number of cycles does not change the morphology of the polymer even if there is γ-Fe_2O_3 in the network polymer. The formation of craters was observed in the composite synthesized with γ-Fe_2O_3 (Figures. 4 d, e, f). However, the films presented cracks as the number of cycles increased.

An accumulation of γ-Fe_2O_3 in the shape of the agglomerates on the surface of the three synthesized composites (Figure. 4 d, e, f) was observed. The films obtained after 15 cycles presented cracks as a structural defect, and because of this, electrochemical measurements were performed with the synthesized composites after 10 cycles. The thickness of the films was determined from cryofracture substrates containing the composite with liquid nitrogen after SEM analysis (not shown). The average size thickness of the composites' thin films was 1.67 ± 0.14 µm, 3.31 ± 0.10 µm, and 6.10 ± 0.63 µm for composites synthesized with 5, 10, and 15 cycles respectively. The SEM of the composites, presented in **Supplementary Data Figure 2 (a)**, showed that the γ-Fe_2O_3 over the composite surface have a nanometer size, while the TEM micrographs of the composite, presented in **Supplementary Data Figure 2 (b)**, show that their diameters were in the range of *ca.* 126 ± 30 nm.

Furthermore, one can observe the presence of magnetite agglomerates in the material evaluated. Some dark spots in **Supplementary Data Figure 2** (**b**) (marked with red arrows) can be seen inside the composite. It can be suggested that these points are γ-Fe_2O_3 nanoparticles.

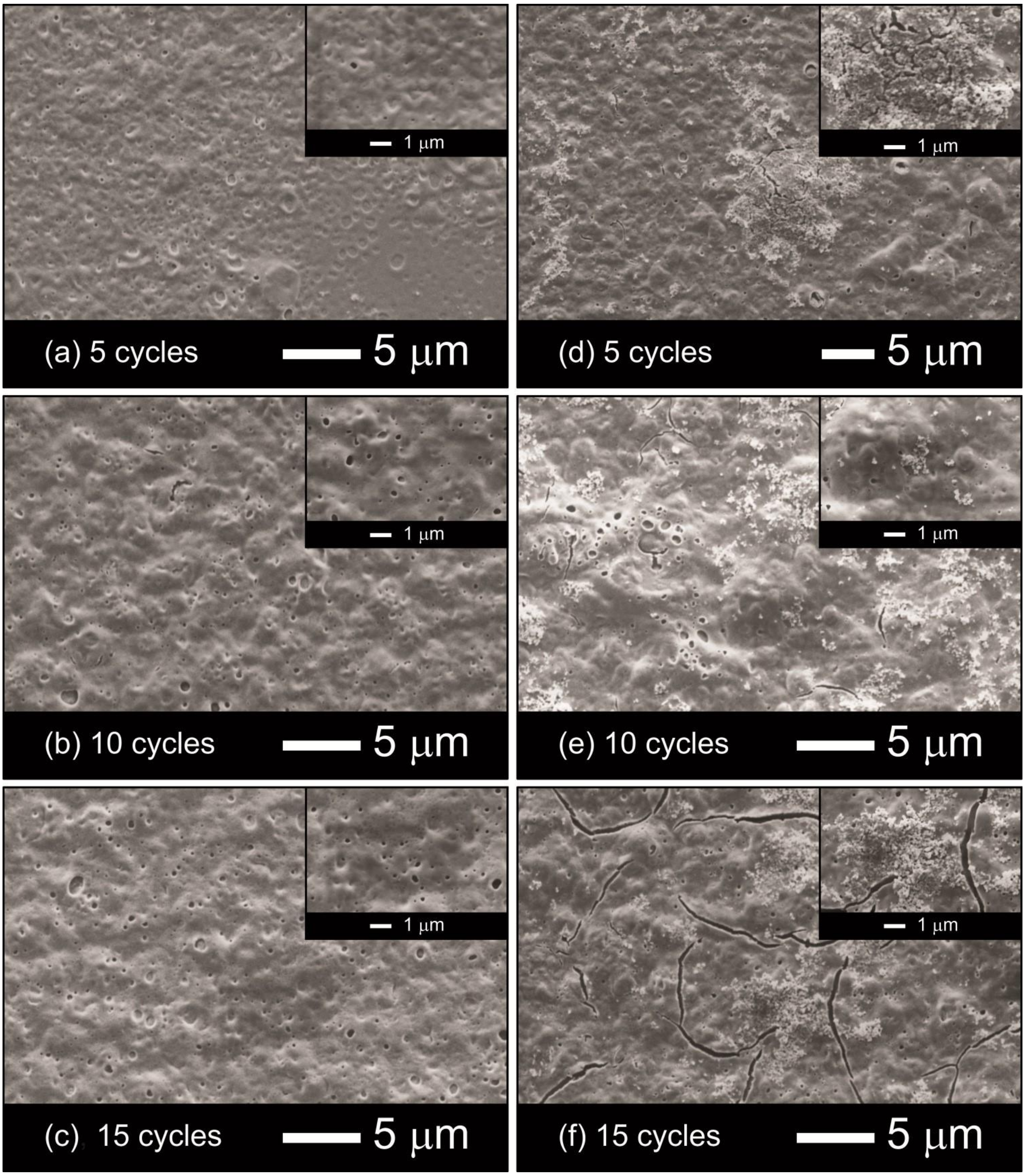

Figure 4. SEM of composites synthesized with oxalic acid and aniline at different deposition cycles (**a**) PANI/OA - 5, (**b**) PANI/OA - 10, (**c**) PANI/OA - 15. Composites synthesized in the presence aniline, oxalic acid and $Fe_2(SO_4)_3$ at different deposition cycles (**d**) PANI/OA/γ-Fe_2O_3 - 5, (**e**) PANI/OA/γ-Fe_2O_3 - 10 (**f**) PANI/OA/γ-Fe_2O_3 - 15.

3.5 Voltammetric study of electrodeposited composite PANI/OA/γ-Fe_2O_3 on the Pt electrode

The electrochemical study allowed us to evaluate the composite electroactivity (PANI/OA/γ-Fe_2O_3). Figure 5 (a) shows cyclic voltammograms registered in NaOH 1.0 mol/L at different scan rates (υ) for the electrodeposited composite, PANI/OA/γ-Fe_2O_3, on the Pt electrode. The voltammograms clearly show that PANI/OA/γ-Fe_2O_3 presents two couples of redox peaks. The first one is at -0.81/-0.84 V and is named couple 1, $E_{pa}1/E_{pc}1$. This is followed by a second one at -0.70/-0.73 V, named couple 2, $E_{pa}2/E_{pc}2$. The anodic and cathodic peak separation (ΔE_p), which is lower than 0.06 V for both couple peaks, suggests that the electrode process has a reversibility characteristic, which can be attributed to the fast electron transfer without kinetic complications [31]. An intensity peak current with irreversible characteristics is observed at -0.35 V, which was attributed to the reduction of Fe^{+3} to Fe^0 as observed by Fosenca *et al.* [3].

The scan rate is an essential experimental parameter that needs to be investigated as the adsorbed film on the electrode surface can be influenced by this parameter. This should be investigated by considering information about the strength of the deposited film. With the result obtained from studying the scan rate, it is also possible to obtain information regarding the electrochemical mechanism and the relationship between the peaks current and the scan rate. Accordingly, the scan rate may influence the electrochemical response of the electroactive composite, PANI/OA/γ-Fe_2O_3, while the voltammetric behavior may result from its effects. The observed peak at -0.35 V presented a linear relationship between the peak current intensity (i_p) and the scan rate (υ) with a regression equation of $i_{pc}(A) = -2.36\times10^{-4} + 6.70\times10^{-6}\ \upsilon(mV/s)$ (n = 12), whose linear correlation coefficient was 0.995. The cathodic peak potential (E_{pc}) was significantly shifted to a more negative value when the scan rate was increased; this was expected, theoretically, for the irreversible process electrode [31]. For all the scan rates (10 - 400 mV/s), the presence of the corresponding anodic peak was not observed in the reverse scan for the well-defined peak at -0.35 V, suggesting an irreversible nature of the electrode process.

For the two couples, $E_{pa}1/E_{pc}1$ and $E_{pa}2/E_{pc}2$, a linear relationship between peak current (i_p) and scan rate (υ) was observed, in which the ratio of the cathodic and anodic peak current (i_{pc}/i_{pa}) was near unity; this was expected, theoretically, for the reversible process [31]. Accordingly, the first one, couple 1 ($E_{pa}1/E_{pc}1$), presented a more interesting effect and was studied for the purpose of this work (Figure 5 b). Accordingly, couple 1 presents a regression equation: $i_{pa}(\mu A) = -2.40\times10^{-4} - 6.70\times10^{-6}\ \upsilon(mV/s)$ and $i_{pc}(\mu A) = -2.10\times10^{-4} + 4.80\times10^{-6}\ \upsilon(mV/s)$ (n = 10), with a linear correlation coefficient of 0.995 and 0.999, respectively, indicating a strong adsorptive electrode process. The current function ($i_p/(\upsilon^{1/2})$, for couples 1 changed with the increasing of the scan rate, and the peak potential values (E_p) shifted slowly to more negative potentials. This behavior also suggested an electrode process with a reversible characteristic [31]. Due to the poor voltammetric profile in a scan rate higher than 400 mV/s, it was impossible to determine the exact values of i_p and E_p for both couples.

Table 1 provides additional information about the electrochemical study of the PANI/OA/γ-Fe_2O_3 at different scan rates. The characteristic parameters for the peaks, i_{pa}, i_{pc}, E_{pa}, E_{pc}, as well as the relation E_p-$E_p/2$, indicate that the composite PANI/OA/γ-Fe_2O_3, electrodeposited at the Pt surface electrode, presents an irreversible process.

According to Fonseca *et al.* [3], who used the electrochemical characteristic of the poly(*o*-anisidine)/γ-Fe_2O_3 (maghemite), the first couple -0.80/-0.84 V and the reduction peak -0.35 V are in agreement with our hypothesis of the composition formation of composite PANI/OA/ γ-Fe_2O_3. This indicates material electroactivity that can be explored further in electrochemical systems or devices for diverse application.

Table 1. Variation of the characteristics parameters for the electrochemical study of the PANI/OA/γ-Fe_2O_3 at different scan rate.

υ $mV\,s^{-1}$	$i_{pa}1$ μA	$E_{pa}1$ V	$i_{pc}1$ μA	$E_{pc}1$ V	$i_{pc}3$ μA	$E_{pc}3$ V	$E_{pa}1-E_{pa}1/2$ V	$E_{pc}1-E_{pc}1/2$ V	$E_{pc}3-E_{pc}3$ V
10					-193	-0.329			-0.095
25					-361	-0.340			-0.107
50	42	-0.814	-35	-0.793	-554	-0.346	0.027	-0.033	-0.100
75	142	-0.806	-118	-0.823	-756	-0.351	0.031	-0.030	-0.103
100	259	-0.804	-218	-0.823	-9367	-0.354	0.035	0.031	-0.103
150	508	-0.803	-435	-0.823	-1288	-0.356	0.040	-0.036	-0.102
175	643	-0.800	-541	-0.822	-1446	-0.358	0.045	-0.034	-0.104
200	766	-0.802	-663	-0.824	-1601	-0.359	0.044	-0.031	-0.100
250	996	-0.800	-874	-0.825	-1915	-0.360	0.046	-0.034	-0.105
300	1250	-0.799	-1070	-0.827	-2439	-0.364	0.052	-0.033	-0.101
350	1480	-0.798	-1230	-0.829	-2476	-0.367	0.051	-0.036	-0.107
400	1710	-0.797	-1430	-0.829	-2764	-0.367	0.053	-0.036	-0.104

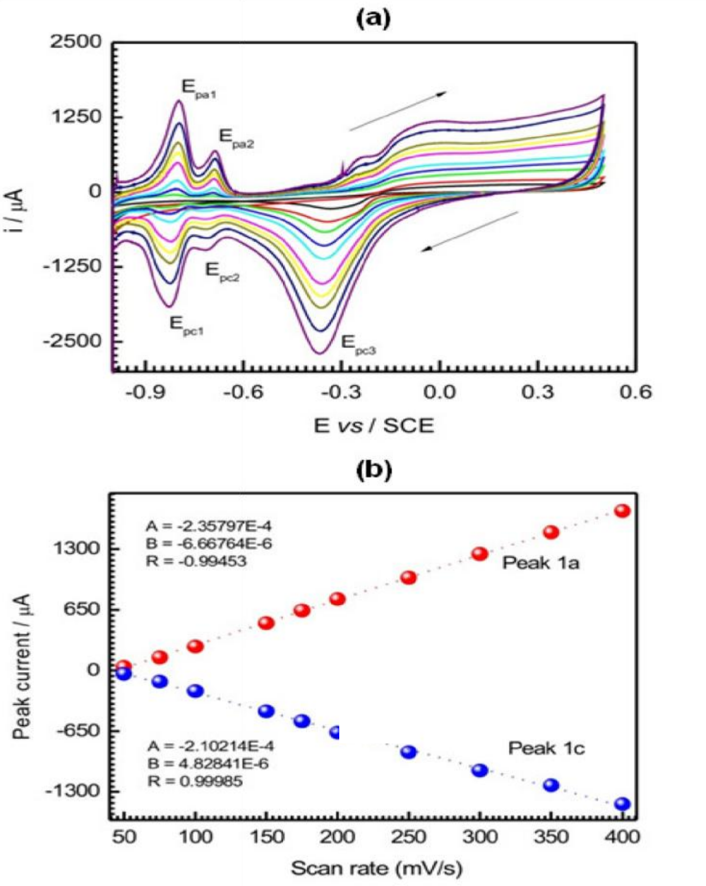

Figure 5. (**a**) The cyclic voltammograms for the composite thin film PANI/OA/γFe_2O_3 – 10 cycles in 1.0 mol/L of NaOH as supporting electrolyte, at various scan rate. (**b**) Dependence of peak current on scan rate variation for the couple 1, $E_{pa}1$ /$E_{pc}1$.

Cyclic voltammetry 100 cycles in HCl 1.0 mol/L was performed to check the stability of the composite (**Supplementary Data Figure 3**). The composite proved to be very stable, and the current density increased with the number of cycles. Two redox pairs are related an anodic peak at 0.48 V and a cathodic peak at 0.30 V are observed. Both redox pairs arose from the oxidation and reduction of the PANI.

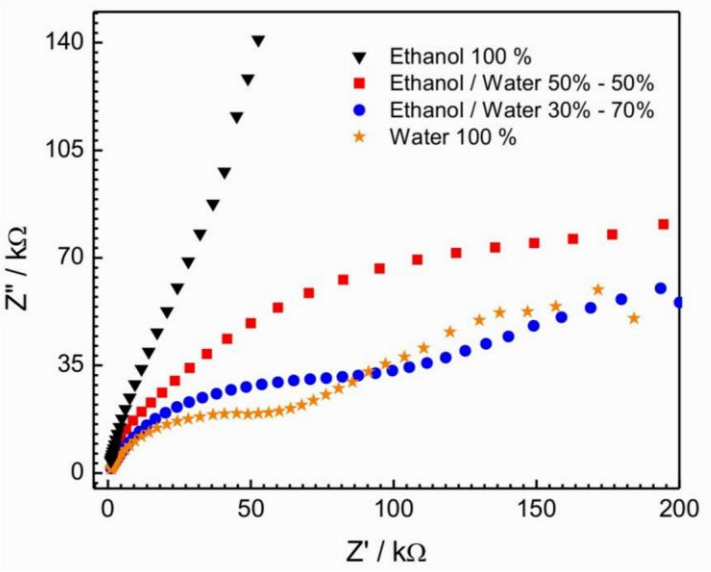

Figure 6. Electrochemical impedance spectroscopy response of hybrid material (PANI/OA/γ-Fe_2O_3 – 10) as a function of percentage of ethanol/water.

The measure of the sensor was realized in a closed bottle (20 mL of volume) with 10 mL of the mixed solvents. The schema of this measure is displayed in **Supplementary Data Figure 4**. The impedance spectra of the composite, presented in Figure 6, in the form of Nyquist plots in ethanol vapor, exhibited a straight line characteristic of a diffusion-limiting step in the electrochemical process. When the composite was exposed to different vapors or to different ethanol mixtures (ethanol/water 70% - 30%) while monitoring the impedance, we observed that the impedance measure decreased and the straight line seemed to become a semicircle characteristic of the limited electron transfer process. In water vapor, 100% of the spectrum obtained the characteristic of a semicircle. The decrease in the resistance of the spectrum, EIE, indicated the material's response to water vapor. The diameter of the semicircle provided an approximate value of the charge-transfer resistance (Rct) at the composite/media interface. The conductivity decrease with the humidity increase is a result of the interaction between water molecules and the metal oxide, presented in this material. As can be seen from Figure 6, the semicircle diameter of PANI/OA/ γ-Fe_2O_3 is much smaller in water vapor than in ethanol. Thus, it is believed that the observed conductivity change in the solution containing higher concentrations of water may be associated with the difference between the properties of the constituents, ethanol/water.

The mechanism by which absorbed water enhances the conductivity is seemingly simple. Water through its ability to make hydrogen links interacts with neighboring ions, and through phenomena involving electrostatic forces freed them to ensure the transport chain. At the same time due to the high dielectric constant of water absorbed, the capacitance of the material increases, resulting in an increase in conductivity that can be available monitored by the sensor.

4. CONCLUSION

The present work efficiently investigated and demonstrated the simultaneous synthesis of the composite thin film PANI/OA/γ-Fe_2O_3 using an electrochemical polymerization method in alkaline media in a single step. The effect of alkaline pH favored the synthesis of metal oxide in a single step, while the efficiency of the synthesis was confirmed by the results reported in this paper. The FT-IR and UV-Vis results demonstrate the formation of the γ-Fe_2O_3-PANI nanocomposite and suggest a synergistic interaction between these nanoparticles and the polymeric matrix of PANI. Due to the presence of γ-Fe_2O_3 nanoparticles, the thermal stability was found to be enhanced compared to pure PANI. The cyclic voltammetry measurements show that the synthesized composite had characteristics of the reversible process. Furthermore, a satisfactory electrochemical stability of the electrodeposited film was observed. Finally, we propose that other works should be performed to identify other materials that could be used as sensors.

ACKNOWLEDGMENTS
Rinaldi thanks Conselho Nacional de Desenvolvimento Científico e Tecnológico—CNPQ (Process: 577527/2008-8 and 310820/2011-1) for financial support. COMCAP – UEM for SEM and TEM analyses.

References

1. E.W. Paul, A.J. Ricco, M.S. Wrighton, *J. Phys. Chem*., 89 (1985) 1441
2. K. D. Balun, K. Fatih, *Appl.Catal., B,* 181 (2016) 88
3. L.H.M. Fonseca, A.W. Rinaldi, A.F. Rubira, L.F. Cótica, S.N. de Medeiros, A. Paesano, I.A. Santos, E.M. Girotto, *Mater. Chem. Phys*., 97 (2006) 252
4. G. Casalbore-Miceli, A. Zanelli, E.M. Girotto, A.W. Rinaldi, A.F. Rubira, A. Berlin, *Electrochim. Acta* 51 (2006) 5268
5. S. Bai, Y. Ma, R. Luo, A. Chen, D. Li, RSC Adv., 6 (2016) 2687
6. T. Kuno, Y. Matsumura, K. Nakabayashi, M. Atobe, *Angew. Chem. Int. Ed.* 55 (2016) 2503
7. J.Z. Ou, S. Balendhran, M.R. Field, D.G. McCulloch, A.S. Zoolfakar, R.A. Rani, S. Zhuiykov, A.P. O'Mullane, K. Kalantar-Zadeh, *Nanoscale* 4 (2012) 5980
8. X. Xia, Q. Hao, W. Lei, W. Wang, D. Sun, X. Wang, *J. Mater. Chem.* 22 (2012) 16844
9. T.H. Ting, R.P. Yu, Y.N. Jau, *Mater. Chem. Phys.* 126 (2011) 364
10. S. Chabungbam, C. G. Loh, M. B. Sahariah, A. R. Pal, R. Pandey, *Chem. Phys. Lett.* 645 (2016) 144
11. S. Ghosh, T. Maiyalaganb, R. N. Basu, *Nanoscale* (2016) DOI: 10.1039/c5nr08803h
12. Y. Liu, J. Li, F. Li, W. Li, H. Yang, X. Zhang, Y. Liuab, J. Ma, *J. Mater. Chem. A.* 4 (2016) 4472
13. N. Menegazzo, D. Boyne, H. Bui, T.P. Jr Beebe, K.S. Booksh, *Anal. Chem*. 84 (2012) 5770
14. B. Shouli, T. Yanli, C. Meng, S. Jianhua, T. Ye, L. Ruixian, C. Aifan, L. Dianqing, *Sens. Actuators, B.* 226 (2016) 540
15. C.L. Yuan, Y.S. Hong, *J. Mater. Sci.* 45 (2010) 3470

16. J. Ding, X. Li, X. Wang, J. Zhang, D. Yu, B. Qiu, *Nanoscale Research Lett,* 10 (2015) 10.1186/s11671-015-1201-z
17. A.C.V. de Araujo, R.J. de Oliveira, S.A. Junior, A.R. Rodrigues, F.L.A. Machado, F.A.O. Cabral, W.M. de Azevedo, *Synth. Met.* 160 (2010) 685
18. J.A. Raj, J. Mathiyarasu, C. Vedhi, P. Manisankar, *Mater. Letters* 64 (2010):895
19. J. Lin, M. Yu, C. Lin, X. Liu, *J. Phys. Chem. C* 111 (2007) 5835
20. D.L. Golié, Z. Brankovié, N. Daneu, S. Bernik, G. Brankovié, *J. Sol-Gel Sci. Technol*. 63 (2012) 116
21. Y. Chen, G. Yang, Z. Zhang, X. Yang, W. Hou, J. Zhu, *Nanoscale* 2 (2010) 2131
22. M. Mumtaz, E. Cloutet, C. Labrugere, G. Hadziioannou, H. Cramail, *Polym. Chem.* 4 (2013) 615
23. C. Zhou, J. Han, G. Song, R. Guo, *Eur. Polym. J*. 44 (2008) 2850
24. X. Peng, F. Luan, X. Liu, D. Diamond, K. Lau, *Electrochim. Acta* 54 (2009) 6172
25. C.T.P. da Silva, M.D.S. Neto, V.L. Lira, S.L. Oliveira, N.L.C. Domingues, A.W. Rinaldi, *Mater. Letters* 100 (2013) 303
26. A. Zanelli, A.W. Rinaldi, Y. Li, M.J. Yang, E.M. Girotto, *Electrochem. Commun.* 11 (2009) 430
27. K.C. Yong, P.J.S. Foot, H. Morgan, S. Cook, A.J. Tinker, *Eur. Polym. J*. 42 (2006) 1716
28. L. Hu, A. Percheron, D. Chaumont, C. Brachais, *J. Sol-Gel Sci. Technol.* 60 (2011) 198
29. T. Hsieh, K. Ho, X. Bi, C. Huang, Y. Wang, Y. Han, Z. Chen, C. Hsu, P. Li, Y. Chang, *Synth. Met.* 160 (2010) 1609
30. S.S. Umare, B.H. Shambharkar, R.S. Ningthoujam, *Synth. Met.* 160 (2010) 1815
31. A.J. Bard, L.R. Faulkner, *Electrochemical methods: Fundamentals and application*, John Wiley & Sons (2000)

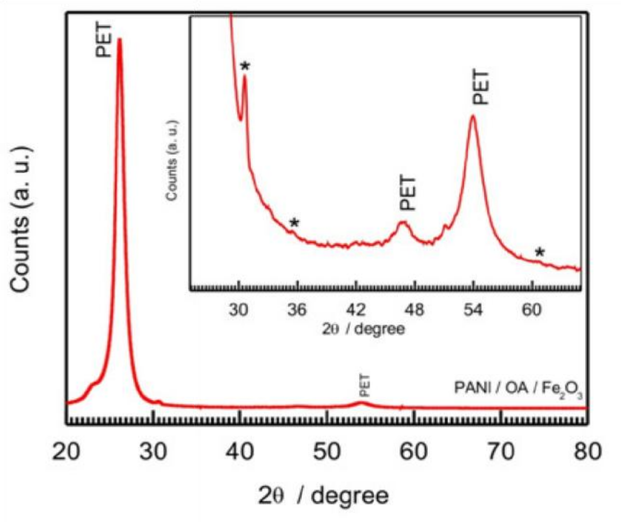

SI. 1 - Supplementary Data Figure 1 – Spectra of X-Ray diffraction of the composite (XRD).

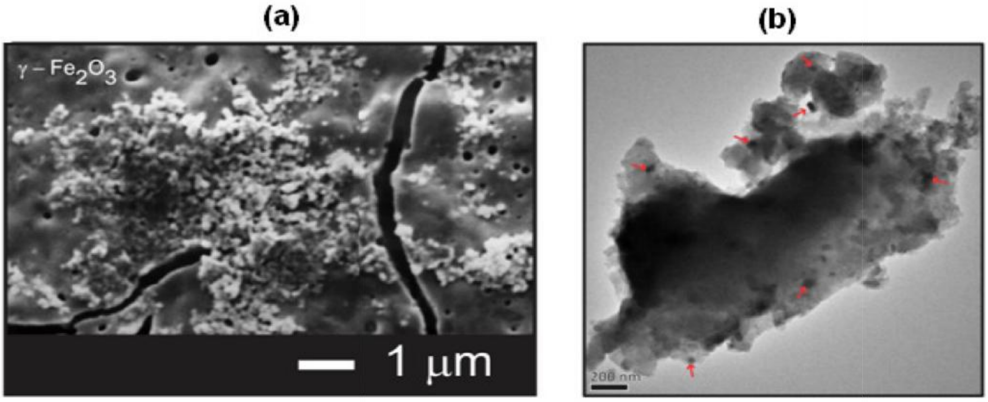

SI. 2 - Supplementary Data Figure 2 – Trasmission Electronic Microscopy of the γ-Fe_2O_3 (**a**), and illustrates the particle size of the materials γ-Fe_2O_3 (**b**).

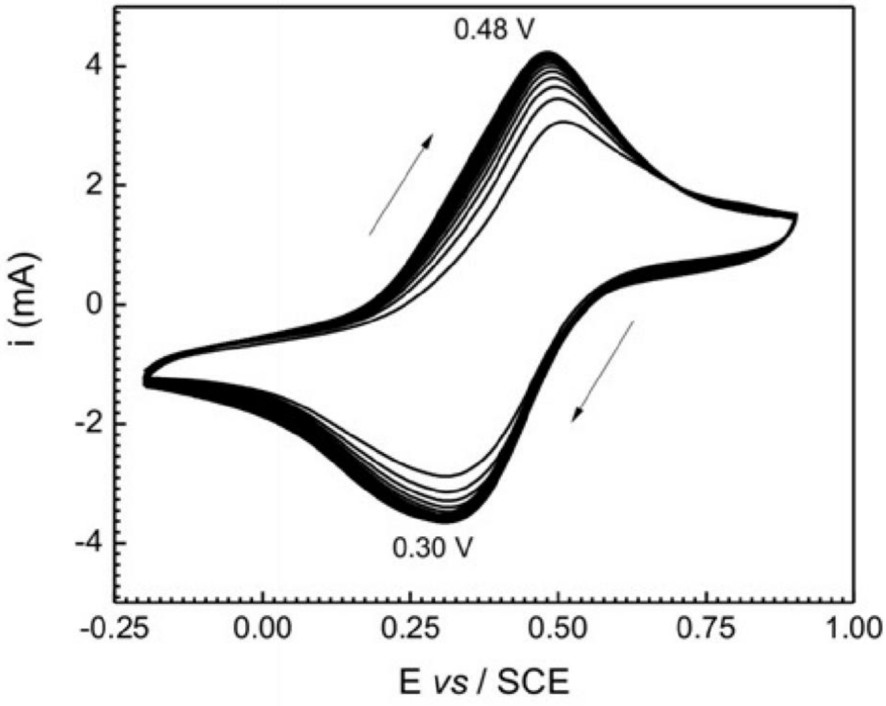

SI. 3 - Supplementary Data Figure 3 – Cyclic voltammetry of the materials. HCl 1.0 mol/L; scan rate 0.10 mV/s; SCE as the reference electrode and 100 cycles.

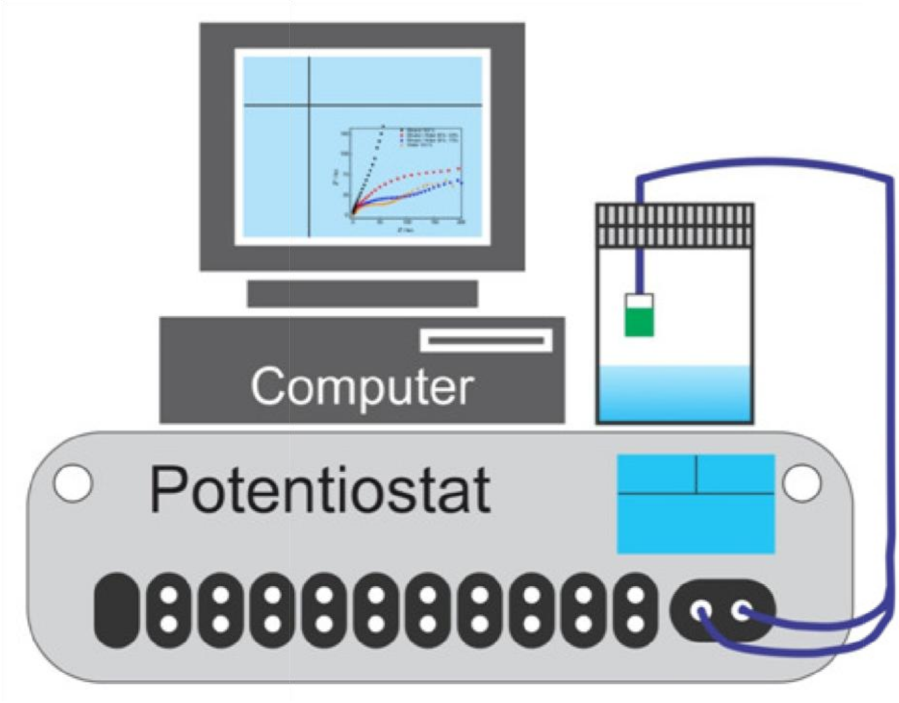

SI. 4 - Supplementary Data Figure 4 – Scheme of this measure.